INTERNATIONAL SOCIETY FOR SOIL MECHANICS AND GEOTECHNICAL ENGINEERING

Analysis of the influence of soft soil depth on the subgrade capacity for flexible pavements.

Analyse de l'influence de la profondeur d'un sol mou sur la capacité portante pour les chaussées souples.

Carvajal E.
Kellerterra S.L., Madrid, Spain

Romana M.
Universidad Politécnica de Madrid, Spain

ABSTRACT: It is presented the analysis of a flexible pavement structure founded on soft soil subgrade, through the finite element modelling of a multilayered system, with the objective to evaluate the influence of soft soil depth on pavement response. The analysis also comprises an iterative procedure to take into account the influence of small strains on soil stiffness. A simple static load of a heavy truck has been used to evaluate the pavement response; furthermore a cyclic loading has been considered in the form of haversine function in order to simulate the traffick effects on cumulative permanent deformation. The results of permanent vertical deformation from the followed procedure is compared to an empirical equation, so that rutting failure intensity is estimated. It is concluded that deep ground treatments should be applied to achieve an allowable capacity of soft soils up to miminum depth of about 6 m, otherwise maintenance cost of pavements might be excessive.

RÉSUMÉ: L'analyse d'une structure de pavement flexible sur un terrain du sol mou est réalisée grâce à une modélisation éléments finis appliquée à un système multicouches. L'objectif est d'évalué l'influence de la profondeur du sol mou sur la réponse de la structure. L'analyse comprend un procédé itératif pour tenir compte de l'influence de petites déformations sur la rigidité du sol. Une charge statique correspondante à un camion poids lourd a été utilisée pour évaluer la réponse du pavement. Une fonction de charge cyclique de type Haversine a été considérée pour simuler les effets de trafic dans la déformation permanente accumulée. Les résultats de la déformation permanente verticale obtenue par cette méthode sont comparés à une équation empirique, pour évaluer l'orniérage. Le constat est la nécessité de traiter sur une profondeur minimum de 6 m le terrain pour atteindre une capacité de charge admissible dans les sols mous. Dans le cas contraire les prix de maintenance et d'entretien des pavements pourraient être excessifs.

KEYWORDS: Pavement, subgrade, cyclic load, permanent deformation, small strain, stiffness, damping ratio, finite element model

MOTS-CLES : pavement, fondation, chargement cyclique, déformation, raideur, amortissement, éléments finis

1 INTRODUCTION.

Flexible pavements over shallow soft soils could be built through the application of a wide range of techniques to improve the low capacity of subgrade, such as lime and cement stabilisation, geogrids and geosynthetic treatments. Nevertheless when the soil layers which compose the subgrade reach certain depths, the intensity of shallow treatments become inefficient and it is necessary to evaluate the depth that is influenced by the load, and the effects on the capacity and long term behaviour of such deep soft subgrade. Here below is presented a theoretical procedure to analyze the response of a flexible pavement on soft soil under static and cyclic loading. It is also presented an estimation of the rut depth failure based on permanent deformation of subgrade layers affected by determined number of load repetitions.

2 PAVEMENTS ANALYSIS

The pavement analysis through mechanistic approaches is increasingly adopted, with the development of numerical modelling tools, considering complex behavior of pavement structure. Actually, because of the amount of variables that have to be dealt, the design of flexible pavements could be divided in two parts, one mechanical and the other empirical, thus nowadays most frequently used methods for the design are often called Mechanstic-Empirical Methods.

The mechanistic part consists on determining the elastic response of the pavement structure in terms of stress, strain and displacement when a heavy truck equivalent load (P) is applied on the surface.The parameters that determine the properties and

thickness of surface layer are radial strain and tensile strain (σ_t ; ε_t) at the bottom of the surface layer. Whereas, the capacity of foundation soil is governed by the vertical compressive stress and deformation in the top of the subgrade (σ_v ; ε_v). Figure 1.

On the other side, the empirical approach is related to relationships between each components of the elastic structural response (σ, ε, y) and a fatigue law. Thus, the damage accumulation for a given number of the load application could be estimated. For this purpose, the fatigue law has to take into account other essential factors that are difficult to assess from the mechanical point of view, e.g. rainfalls, temperature changes, drainage conditions, etc. Particularly, the evaluation of pavement foundation (subgrade layers) is usually estimated through an allowable number of load repetitions (Nd) that produces unacceptable permanent deformation, which is commonly known as rutting failure mechanism. Otherwise, after construction stage settlements produced due to weight of fills and pavement structure has to be considered, although, even more important matter will be estimation of the time of consolidation process and determination of the soils stress state after consolidation and at the begining of traffic operation.
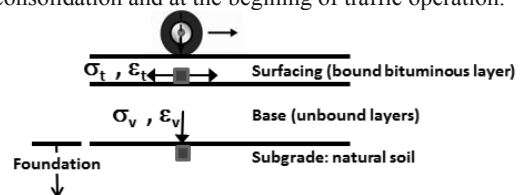

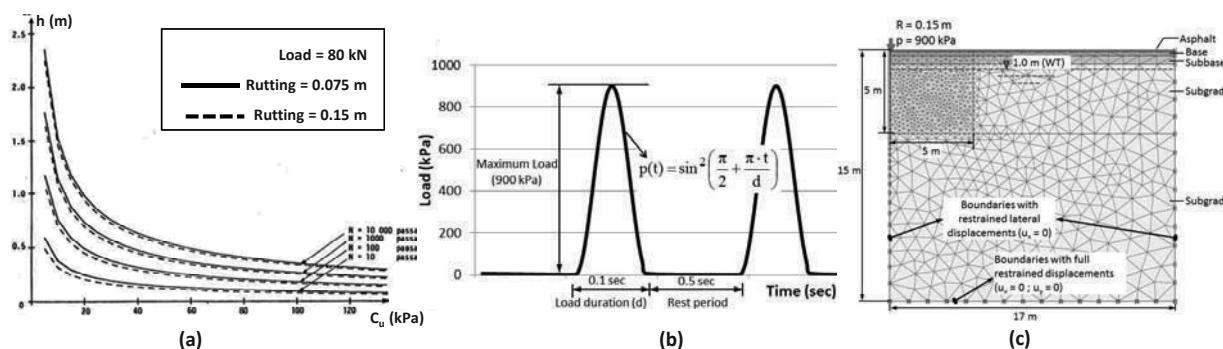Figure 1. Parameters for pavement design

Figure 2. (a) Base layer thickness as a function of subgrade undrained shear strength, number of load application (80 kN) and rut depth (Giroud and Noiray 1981); (b) cyclic load used for finite element modelling; (c) geometry of finite element model.

Figure 2a shows a chart proposed by Giroud and Noiray (1981) to select the required thickness of un-reinforced granular layer, which provides an allowable rut depth on unpaved roads. This chart shows that even for low trafficked road it is required a ganular thickness larger than 1 m when subgrade soil presents undrained shear strenght less than $C_u = 20$ kPa, and number of load application N is greater than 10000. With more greater N and less values of Cu, base layers tend to be too large. In these cases the settlements after construction stage and the consolidation periods may be unacceptable.

3 MODELLING OF SOFT SUBGRADE

3.1 Introduction

A theoretical procedure to estimate the structural response of a pavement founded over a deep soft subgrade is presented, focusing on vertical stresses and strains within the subgrade. For this purpose a mechanistic finite element model has been performed with the program Plaxis v8.2, considering the pavement structure depicted in Figure 2c. The analysis is separately presented according to static and cyclic load conditions, and basically is focused on the influence of subgrade behavior. Accordingly only stresses and strains regarding subgrade layers will be analyzed.

3.2 Geometry and general inputs

The pavement modelling is carried out with axisymmetric conditions for a multi-layered system composed by an asphalt surface layer, followed by two unbound granular layers as base and subbase. A subgrade composed by natural soil is adopted below pavement structure considering the water table at 1 m depth. Vertical boundaries are restrained for lateral displacements, while the bottom horizontal boundary is full restrained for both lateral and vertical displacements. It was adopted an extra-fine mesh of 15-noded elements close to upper part of the model axis, where loading is applied. All of materials constituting the pavement superstructure are modeled as linear elastic, so that the required parameters are only the young modulus E and Poisson's ratio ν. In Table 1 are outlined the parameters of pavement superstructure.

Table 1. Parameters of asphalt layer and unbound granular layers

Layer	Thickness m	E kPa	ν
Asphalt	0.1	$1.3 \cdot 10^6$	0.2
Base	0.25	$1.5 \cdot 10^5$	0.33
Subbase	0.5	$1 \cdot 10^5$	0.33

On the other hand, isotropic hardening soil behavior is considered for the subgrade, which is governed by a stress-dependent stiffness that is different for both virgin loading and unloading-reloading process (Schanz 1998). The hardening soil model may be considered as an extension of the well known hyperbolic model (Duncan and Chang 1970), owing to the use of plasticity theory and yield cap surface to account for the hardening effect produced by isotropic compression strains. The parameters adopted for the soft subgrade soil are presented in Table 2., and its characterization is in accordance with the stiffness increase due to the typical small strains that affects pavement performance.

Table 2. Parameters of subgrade soil

Parameter	Symbol	Values	Unit
Unit weight	γ	16.5	kN/m³
Small Strain stiffness	G_0^{ref}	45000	kN/m²
Shear strain at $0.7G_0$	$\gamma_{0.7}^{ref}$	$1.75 \cdot 10^{-4}$	-
Poisson's ratio	ν_{ur}	0.3	-
Triaxial compression stiffness	E_{50}^{ref}	10000	kN/m²
Primary oedometer stiffness	E_{oed}^{ref}	10000	kN/m²
Unloading - reloading stiffness	E_{ur}^{ref}	20000	kN/m²
Rate of stress-dependency	m	0.85	
Cohesion	c'	5	kN/m²
Friction angle	ϕ'	10	°
Failure ratio ($q_f/q_{asymptote}$)	R_f	0.9	-
Stress ratio in primary compression	K_0^{nc}	0.83	-

The parameter G_0 and $\gamma_{0.7}$ are used in order to consider the variation of moduli at small strains, as describe below.

The load condition has been evaluated by means of a static surcharge, which represents the application of a single axle load of 13 t, with a contact area of 0.15 m radius, so that maximum pressure on the surface reaches up to 900 kPa. The cyclic loading conditions have been performed considering a waveform pattern in order to simulate the accumulation of permanent deformation. Thereby, it is assumed a stress pulse over the pavement surface in the form of a haversine function, which may be defined by the use of an equivalent pulse time of 0.1 second, associated to a vehicle speed of 30 km/h (Barksdale 1971). Figure 2b shows the cyclic load pulse adopted.

3.3 Modelling procedure

The calculation consists of one stage that is related to the pavement construction, where unbound granular and asphalt layers are laid out over the subgrade soil. Following stage consist of cyclic load application, in order to simulate the action of traffic. Initially, no drained condition is assumed for two stage considered. After the load application a consolidation phase is included to take account of the final stress state and to evaluate the time of the pore-pressure dissipation.

The effects of cyclic loading on the pavement behavior are analyzed in several steps in order to consider the influence of strain level and the soil damping on the pavement response. Thus, it is adopted an iterative procedure to consider the updating of the soil stiffness according to the strain level during the cyclic loading. This procedure was performed through the stoppage of the loading process once 10 cyclic of load repetition completed, determining the average values of shear strains related to the subgrade layers. In order to update the actual

stress state after load repetitions, overconsolidation ratio OCR of natural soft soil is systematically recalculated due to the modification of the stress history. In total 10 iterations of cyclic loading have been adopted with 10 load repetition each one, so that the analysis reaches 100 load applications.

The decrease of clay stiffness due to increase of the load repetitions is well known issue. To take into account this effect Idriss et al. (1978) proposed that the decrease in modulus could be accounted for by a degradation index δ according to (1).

$$\delta = (E_S)_N / (E_S)_1 = N^{-t} \qquad (1)$$

Where: $(E_S)_N$ is the secant young's modulus for Nth cycle; $(E_S)_1$ is the secant young's modulus for the first cycle; and t is a degradation parameter, which represent the slope of the curve $\log E_S - \log N$.

On the other hand, in order to take into account the influence of the typical small strains produced below the pavement structures, it was assumed the soil stiffness degradation due to strain level. Hardin and Drnevich (1972) proposed a simple hyperbolic law to describe how the shear modulus of soil decays with the increase of shear strains. Afterward, Santos and Gomes Correia (2001) modified this relationship to determine de variation of secant shear modulus G_S as a function of the initial (and maximum) shear modulus at small strains G_0, and of the shear strain $\gamma_{0.7}$ related to the 70% of the maximum shear modulus $0.7G_0$ as a threshold. Equation 2 describes this relation in the domain of a certain range of shear strain, commonly within values from $1 \cdot 10^{-6}$ to $1 \cdot 10^{-2}$. The tangent shear modulus G_t can be determined taking the derivative of G_S.

$$G_S = \frac{G_0}{1 + 0.385 \cdot (\gamma/\gamma_{0.7})} \quad ; \quad G_t = \frac{G_0}{(1 + 0.385 \cdot (\gamma/\gamma_{0.7}))^2} \qquad (2)$$

This approach is based on the research carried out by Vucetic and Dobry (1991) and Ishihara (1996), which demonstrated that beyond a volumetric threshold strain γ_v the soil starts to change irreversibly. At this strain level, in drained conditions permanent volume change will take place, whereas in undrained conditions pore water pressure will build up (Santos and Gomes Correia 2001). Furthermore, it is well known that the degradation of G/G_0 with shear strains depends on many factors e.g. plasticity index, stress history, effective confine pressure, frequency and number of load cycle, etc. Indeed, with the purpose of consider the influence of the most importance factors on the degradation of shear moduli, Santos and Gomes Correia (2001) used the average value of γ_v related to the stiffness degradation curves ($G/G_0 = f(\gamma)$) presented by Vucetic and Dobry (1991), in order to define a unique curve of G/G_0 as a function of normalized strain γ/γ_v. In this way they concluded that when the ratio $\gamma/\gamma_v = 1$ the best fit tends to correspond to a ratio $G/G_0 = 0.7$.

This approach aids to develop the small-strain stiffness model (HSsmall) proposed by Benz (2006) that is already included in the latest version of Plaxis code. Unlike the standard Hardening Soil Model (Schanz et al. 1999) where a linear stress strain relationship controlled by the stiffness E_{ur} is assumed during unloading-reloading process, the HS-small model takes into account hysteresis loops during loading and unloading cycles with moduli variation among initial E_0, secant E_{50} and unloading-reloading E_{ur} stiffness (Figure 3). In fact, such model also presents a typical hysteretic damping when the soil is under cyclic loading due to energy dissipation caused by the strains; Brinkgreve et al (2007) proposed an analytical formulation to estimate the local hysteretic damping ratio according to Equation 3:
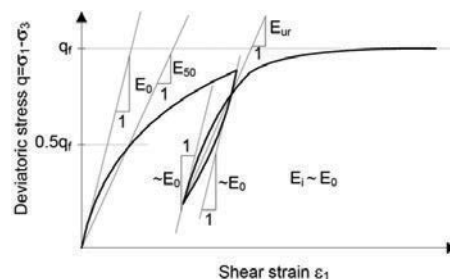

Figure 3. Hyperbolic stress-strain relation and moduli E_0, E_{50} and E_{ur} adopted in the HS-small model.

$$\xi = E_D / 4 \cdot \pi \cdot E_S \qquad (3)$$

Where E_D is the dissipated energy in a load cycle comprised from the minimum to maximum shear strain (Equation 4), while E_S is the energy stored at maximum shear strain γ_c (Equation 5).

$$E_D = \frac{4\gamma_{0.7}G_0}{a}\left(2\gamma_c - \frac{\gamma_c}{1+\gamma_{0.7}/a\gamma_c} - \frac{2\gamma_{0.7}}{a} \cdot \ln\left(1 + \frac{a\gamma_c}{\gamma_{0.7}}\right)\right) \qquad (4)$$

$$E_S = \frac{1}{2}G_S\gamma_c^2 = \frac{G_0\gamma_c^2}{2 + 2a\gamma_c^2/\gamma_{0.7}} \qquad (5)$$

Where $a = 0.385$

Once assumed the calculation procedure described above, the hysteretic damping ratio according to Equation 3 is estimated from the strain updating after each iterative calculation (10 iterations each consisting of ten load repetitions), considering the calibration of soil stiffness due to strain level (γ), current stress state (OCR) and number of load repetitions (N). Moreover, viscous damping effects may be added by means of the rayleigh damping features of the used Plaxis version (v8.2). Rayleigh damping consists in a frequency-dependent damping that is directly proportional to the mass and the stiffness matrix through the coefficients α and β respectively ($C = \alpha \cdot M + \beta \cdot K$). In fact, the damping process subjected to a cyclic loading should be analyzed from the combination of two approaches: mechanical hysteretic damping depending on the strains level, and viscous damping depending on the time, which has to fit well with both, natural material and load application frequency. For this purpose the values adopted for Rayleigh coefficients are $\beta = \alpha = 0.01$.

As small-strain stiffness model is not included in the version 8.2 of Plaxis code used here, the analytical solution of Brinkgreve et al (2007) is adopted to verify and compare the damping ratios between the results from the finite element modeling and the results from such analytical solution. Finally, the behavior of subgrade soil is analyzed regarding the accumulated vertical strains due to the cyclic load repetitions.

3.4 Modelling results

3.4.1 Subgrade response under static loading

The settlement after construction stage rise up to 25 mm, which should last less than few months according to the typical projects requirements. Nevertheless, the consolidation process may lasts between 1.5 to 2.5 years considering a soil permeability of 10^{-8} to 10^{-9} m/s. Regarding the operation stage, the maximum value of excess pore pressure due to axle load rises up to 5.5 kPa. The response of subgrade soil when the axle load is applied under static conditions can be appreciated through the values of deviator stresses as well as vertical resilient and permanent strains depending on the depth (Figure 4a).
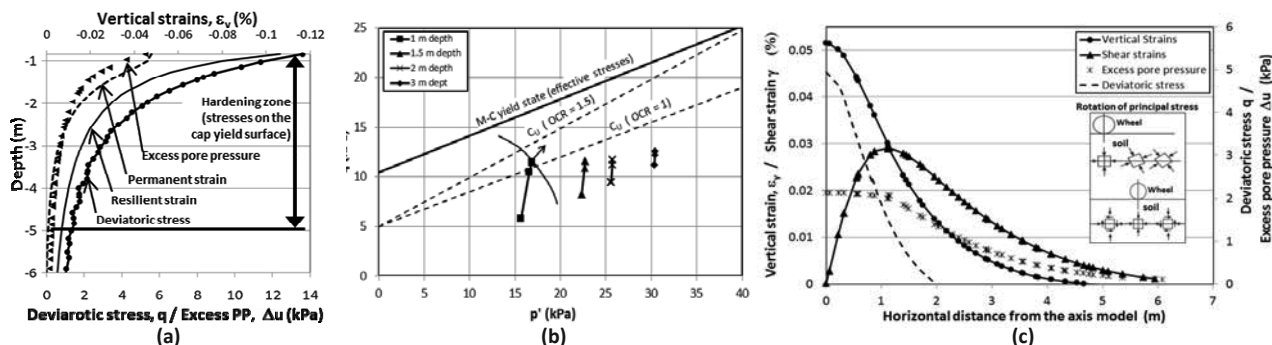
Figure 4. Subgrade response under static loading; (a) deviator stress, permanent and resilient strains, and excess pore pressure; (b) stress state at different depths and failure criteria under drained and undrained conditions;(c) horizontal distribution of stresses and strains at 1.5 m depth.

The influence of axle load below pavement surface reaches 6 m depth, although the most of strains take place in the upper layers of subgrade.

It is also noted that within upper 5 m the stresses reaches cap yield surface, leading to an isotropic hardening of soil. Besides, Figure 4b shows the stress states at different depths, where can be seen that the current effective stress state remains far of Mohr Coulomb failure condition, although it is near the undrained failure e.g. according to the empirical equation $S_u = 0.35 \cdot \sigma_v' \cdot OCR^m$ proposed by Ladd (1991), with $OCR = 1$ and $m = 0.85$. The ratio between current deviator stress and deviator stress at failure $R = q/q_f$ could be used to express the extent to which permanent deformation might develops; usually it is assumed that permanent deformation will start to rise for $R > 0.70 – 0.75$ (Korkiala-Tanttu 2008). In any case, isotropic compression produces plastic volume strains once the excess pore pressures are completely dissipated.

The horizontal distribution of shear and vertical strains at 1.5 m depth are shown in Figure 4c; it can be seen that in the vertical axis, there is no shear strains and the vertical strain reaches its maximum value, which indicates a purely triaxial compression state just below the load. On the other hand, the largest shear strain is located at a horizontal distance of 1.10 m from the load, where soil is under a general stress regime with shear and axial stresses. In reality, when cyclic load of moving wheel over the pavement surface is applied, these two stress state are successively changed. Also it is noted that at 1.5 m depth the maximum deviator stress reaches values near 6 kPa, and spreads horizontally up to 2 m from the load axis. Whereas the influence of excess pore pressure spreads horizontally until 4.5 m, approximately.

3.4.2 Subgrade response under cyclic loading

The effect of one cyclic loading stage composed by 10 load repetitions is shown in Figure 5; the deviator stress, as well as recoverable and permanent displacement at different depths are also depicted in Figure 5. In Figure 6a are shown the curves of shear moduli degradation G_S/G_0 and G_t/G_0 determined by the Equation (2) as a function of strain level and the parameters G_0 and $\gamma_{0.7}$ outlined in the table 1. Also in Figure 6a are shown the results of finite element modelling for the maximum shear strains produced after each iterative calculus under cyclic loading, for a reference depth of 1.5 m. The interception of these maximum shear strains with the curves G_S/G_0 and G_t/G_0 gives the proportion at which soil modulus is changed.

In a next step, stiffness are reduced due to number of load repetitions by means of Equation 1, considering a parameter $t = 0.045$ (Dobry and Vucetic 1987).

It was observed that maximum shear strain obtained in the first 10 load repetitions ($\gamma = 2.9 \cdot 10^{-4}$) is larger than the reference shear strains $\gamma_{0.7}(1.75 \cdot 10^{-4})$, which coincides with the proportion of permanent deformation at this loading stage. After 20 load repetitions the shear strain was lower than the $\gamma_{0.7}$, and after the subsequent load repetitions the strains were reduced more

slowly until reach values leading to ratios $G_S/G_0 = 0.82$ and $G_t/G_0 = 0.67$. The OCR was gradually increased in between each iterative calculation up to a maximum value of 1.50. In the Table 3 are shown the results of final subgrade soil stiffness at a reference depth of 1.5 m.

The damping ratio obtained from the adopted procedure is verified according to the Equations (3) to (5), taking the maximum shear strain after each iteration, in order to reproduce a representative hysteresis loop. Thus, in total 10 damping ratios have been estimated. In Figure 6b are shown the results of damping ratio compared to the analytical results for hysteretic damping considering variation of initial shear modulus G_0 from values of $2G_{ur}$ to $6G_{ur}$, and variation of $\gamma_{0.7}$ from $1 \cdot 10^{-4}$ to $2 \cdot 10^{-4}$.

It is observed that results obtained from finite element modelling fit well with hysteretic damping related to $\gamma_{0.7} = 1.75 \cdot 10^{-4}$. In the two first iterations was obtained damping ratios close to 0.1, which were reduced gradually until the final iterations reached values close 0.045. This tendency agrees with the typical reduction in the amount of permanent deformation with the load repetitions, due to the reduction in the amount of dissipated energy.
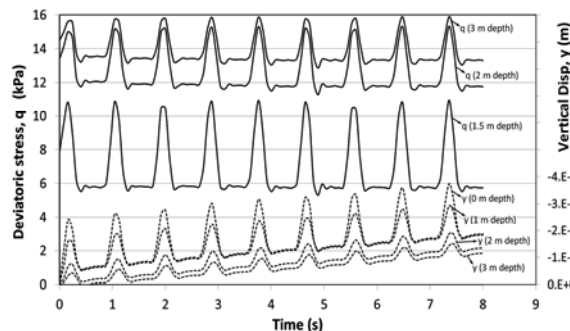

Figure 5. Subgrade response under cyclic loading.

3.4.3 Subgrade performance in the long term

In order to estimate the long term behavior of the soft subgrade analyzed, one could adopt an empirical power equation for calculating the cumulative plastic strain. Chai and Miura (2000) proposed an enhanced formula of a former empirical model proposed by Li and Selig (1996) for estimation of cumulative plastic strains with the number of repeated load applications. This new model is defined in the Equation (6), which has demonstrated that its prediction agrees with actual measurements taken from low height embankments on soft soil.

$$\varepsilon_p = a \cdot (q_d/q_f)^m \cdot (1 + q_{is}/q_f)^n \cdot N^b \qquad (6)$$

Where ε_p = cumulative plastic strain (%); q_{is} = initial static deviator stress; q_d = dynamic load induced deviator stress;
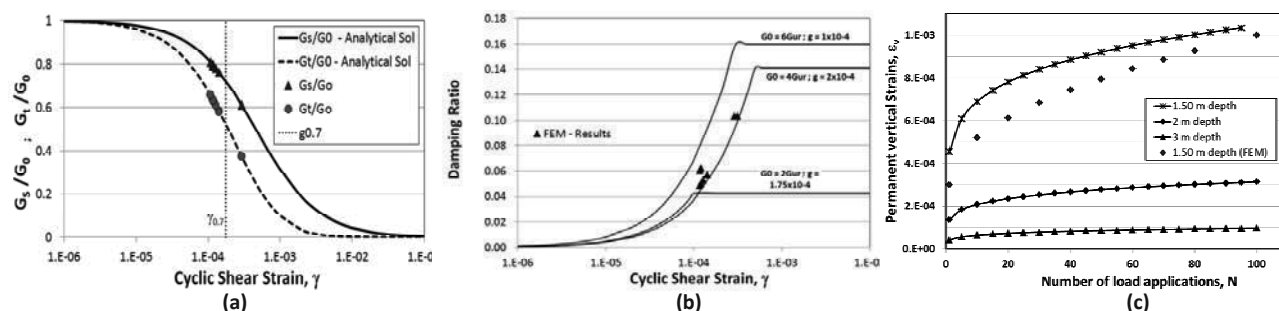
Figure 6. (a) Shear moduli variation with strain level; (b) damping ratio according to cyclic shear strain; (c) cumulative strain with load repetitions.
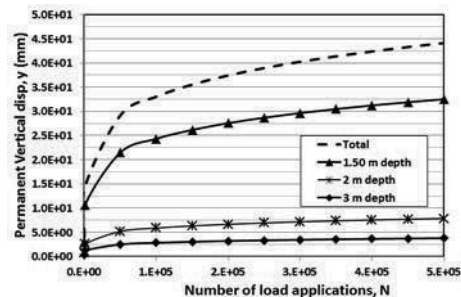

Figure 7. Cumulative vertical displacement (rutting depth).

q_f = static failure deviator stress; N = number of repeated load applications; and a, m, n and b are constant largely dependant on soil properties, which could be assumed for the soft soil analyzed here, according to those values suggested by Li and Selig (1996): a = 1.2; b = 0.18; m = 2.4; n = 1.

Considering the results of q_{is}, q_d and q_f depicted in Figures 4b and 5, the cumulative plastic strain is calculated at different depths according to the Equation 6. In Figure 6c is observed that results from finite element model fit reasonably well with the empirical equation proposed by Chai and Miura (2000) considering N = 100. Otherwise, Figure 7 shows a cumulative permanent deflection of about 45 mm (rut depth), given from Equation 6 for a number of repeated load applications up to N = $5 \cdot 10^5$, and considering the thickness of soft soil influenced by the cyclic load. Such results suppose an unallowable level of rutting failure, even for a low trafficked road as its typical thresholds range from 10 to 15 mm for N greater than 10^6. Possible solutions for pavements based over such soft soil might be achieved by means of deep ground improvement, which could overcome the detrimental effects of the induced deviator stress and excess pore pressure throughout the depth of load influence (Elias et al. 2004, Sonderman and Wehr 2004).

Table 3. Results of subgrade soil stiffness at 1.5 m depth.

Parameter	Unit	Number of load repetitions			
		10	30	50	100
OCR	-	1.2	1.4	1.47	1.5
γ	-	2.90E-04	1.16E-04	1.20E-04	1.07E-04
G_s/G_0	-	0.61	0.80	0.79	0.81
G_t/G_0	-	0.37	0.63	0.63	0.66
G_S	kPa	27473	35851	35601	29485
δ	-	0.891	0.844	0.822	0.794
$E_{ur}*$	kPa	63661	78635	73191	58551
$E_{50}*$	kPa	25464	31454	29276	23421

*final stiffness

4 CONCLUSION

The theoretical procedure presented by means of finite element modelling has shown that deep soft soils might be decisive to long term behavior of flexible pavements, especially in the cases when shallow treatments of subgrade would be uneconomic or inefficient. Deep soil treatments should be applied to achieve an allowable capacity of soft soils up to minimum depth of about 6 m, otherwise maintenance cost of pavements might be excessive. The analysis presented has included the response of soft subgrade layers under static and cyclic loading taking into account the influence of small-strain levels on the soil stiffness; the results fit reasonably well with the analytical solution of hysteretic damping ratio presented by Brinkgreve et al. (2007).

5 REFERENCES

Barksdale R. G. 1971. Compressive stress pulse times in flexible pavements for use in dynamic testing. Highway Research Record 345. pp 32-44. Highway Research Board.

Benz T. 2006. Small-strain stiffness of soils and its numerical consequences. Ph.d. thesis. Universität Stuttgart.

Brikgreve R. B. J. Kappert M.H. and Bonnier P.G. 2007. Hysteretic damping in a small-strain stiffness model. NUMOG X. 737-742.

Chai J. C. and Miura N. 2000. Traffic load induced permanent deformation of low road embankment on soft subsoil. Proceedings of International Conference on Geotechnical and Geological Engineering. CD Rom, Paper No. DE0239

Dobry R. and Vucetic M. 1987. Dynamic properties and seismic response of soft clay deposits. Proc. International Symposium on Geotechnical Engineering of soft soils. Mexico city. pp 51-87.

Duncan J.M. and Chang C.Y. 1970. Nonlinear analysis of stress and strain in soil. J. Soil Mech. Found. Div. ASCE 96. 1629-1653.

Elias V. Welsh J. Warren J. Lukas R. Collin J.G. and Berg R.R. 2004. Ground Improvement Methods. Participant Notebook. NHI Course 132034. FHWA NHI-04-001. Washington. D.C. 1022 pp.

Giroud J.P. and Noiray L. 1981. Geotextiles-reinforced unpaved road design. ASCE. Journal of Geotech. Engg. 107(9). 1233-1253

Hardin B. O. and Drnevich V. P. 1972. Shear modulus and damping in soils: Design equations and curves. Proc. ASCE: Journal of the Soil Mechanics and Foundations Division. 98(SM7). 667-692.

Idriss I. M. Dobry R. and Singh R.D. 1978. Nonlinear behavior of soft clays during cyclic loading. Journal of Geotech. Engg. ASCE. vol. 104. No. GT12. Dec. pp. 1427-1447.

Ishihara K. 1996. Soil Behaviour in Earthquake Geotechnics. Oxford Engineering Science Series. Oxford University Press.

Korkiala-Tanttu L. and Laaksonen R. 2004. Modelling of the stress state and deformations of APT tests. In Proc. of the 2nd Int. Conf. on Accelerated Pavement Testing. Minnesota. Worel, B. 22 p.

Ladd C. C. 1991. Stability evaluation during stage construction. Journal of Geotechnical Engineering. ASCE. Vol. 117. No. 4. pp. 541-615.

Li D. and Selig E.T. 1996. Cumulative plastic deformation for fine-grained subgrade soils. Journal of Geotechnical Engineering. ASCE. Vol. 122. No. 12. pp. 1006-1013.

Santos J. A. and Correia A.G. 2001. Reference threshold shear strain of soil. Its application to obtain a unique strain-dependent shear modulus curve for soil. Proc. 15th Int. Conf. on Soil Mechanics and Geotechnical Engg. Istanbul. Vol 1. 267-270.

Schanz T. 1998. Zur Modellierung des Mechanischen Verhaltens von Reibungsmaterialen. Habilitation. Stuttgart Universität.

Schanz T. Vermeer P.A. and Bonnier P.G. 1999. The hardening-soil model: Formulation and verification. In R.B.J Brinkgreve. Beyond 2000 in Computational Geotechnics. Balkema. Rotterdam. 281-290.

Sonderman W. and Wehr W. 2004. Deep vibro techniques. In Moseley M.P. and Kirsch K. eds. Ground Improvement 2nd edition. Spon Press. London and New York.

Vucetic M. and Dobry R. 1991. Effect of soil plasticity on cyclic response. Journal of Geotech. Engg. ASCE. vol. 117. pp. 89-107.